PHYSICAL REVIEW D **86,** 023517 (2012)

Cosmological lepton asymmetry with a nonzero mixing angle θ_{13}

Emanuele Castorina,[1] Urbano França,[2] Massimiliano Lattanzi,[3] Julien Lesgourgues,[4,5,6]
Gianpiero Mangano,[7] Alessandro Melchiorri,[8] and Sergio Pastor[2]

[1]*SISSA, Via Bonomea 265, 34136, Trieste, Italy*
[2]*Instituto de Física Corpuscular (CSIC-Universitat de València), Apartado 22085, 46071 Valencia, Spain*
[3]*Dipartimento di Fisica G. Occhialini, Università Milano-Bicocca and INFN, Sezione di Milano-Bicocca, Piazza della Scienza 3, I-20126 Milano, Italy*
[4]*CERN, Theory Division, CH-1211 Geneva 23, Switzerland*
[5]*Institut de Théorie des Phénomènes Physiques, EPFL, CH-1015 Lausanne, Switzerland*
[6]*LAPTH (CNRS-Université de Savoie), Boîte Postale 110, F-74941 Annecy-le-Vieux Cedex, France*
[7]*INFN, Sezione di Napoli, Complesso Universitario Monte S. Angelo, Via Cintia, I-80126 Napoli, Italy*
[8]*Physics Department and INFN, Università di Roma La Sapienza, Ple Aldo Moro 2, 00185, Rome, Italy*

(Received 30 April 2012; published 10 July 2012)

While the baryon asymmetry of the Universe is nowadays well measured by cosmological observations, the bounds on the lepton asymmetry in the form of neutrinos are still significantly weaker. We place limits on the relic neutrino asymmetries using some of the latest cosmological data, taking into account the effect of flavor oscillations. We present our results for two different values of the neutrino mixing angle θ_{13}, and show that for large θ_{13} the limits on the total neutrino asymmetry become more stringent, diluting even large initial flavor asymmetries. In particular, we find that the present bounds are still dominated by the limits coming from big bang nucleosynthesis, while the limits on the total neutrino mass from cosmological data are essentially independent of θ_{13}. Finally, we perform a forecast for Cosmic Origins Explorer, taken as an example of a future cosmic microwave background experiment, and find that it could improve the limits on the total lepton asymmetry approximately by up to a factor 6.6.

DOI: 10.1103/PhysRevD.86.023517 PACS numbers: 98.80.−k, 14.60.Pq, 26.35.+c, 98.70.Vc

I. INTRODUCTION

Quantifying the asymmetry between matter and antimatter of the Universe is crucial for understanding some of the particle physics processes that might have taken place in the early Universe, at energies much larger than the ones that can be reached currently in particle accelerators. Probes of the anisotropies of the cosmic microwave background (CMB) together with other cosmological observations have measured the cosmological baryon asymmetry η_b to the percent level thanks to very precise measurements of the baryon density [1]. For the lepton asymmetries, while they are expected to be of the same order of the baryonic one due to sphaleron effects that equilibrate both asymmetries, it could be the case that other physical processes lead instead to leptonic asymmetries much larger than η_b (see, e.g., [2–4]), with consequences for the early Universe phase transitions [5], cosmological magnetic fields [6], and the dark matter relic density [7–9]. Neutrino asymmetries are also bound to be nonzero in the presence of neutrino isocurvature perturbations, like those generated by curvaton decay [10–12]. Those large neutrino asymmetries could have been imprinted in the cosmological data [13,14], and although the limits on such asymmetries have been improving over the last years, current constraints are still many orders of magnitude weaker than the baryonic measurement.

On the other hand, thanks to the neutrino oscillations the initial primordial flavor asymmetries are redistributed among the active neutrinos before the onset of big bang nucleosynthesis (BBN) [15–17], which makes the knowledge of the oscillation parameters important for correctly interpreting the limits on such asymmetries. Nowadays all of those parameters are accurately measured (see e.g. [18,19]), with the exception of the mixing angle θ_{13} that only recently started to be significantly constrained. In fact, several neutrino experiments over the last year gave indications of nonzero values for $\sin^2\theta_{13}$ [20–22], and recently the Daya Bay reactor experiment claimed a measurement of $\sin^2(2\theta_{13}) = 0.092 \pm 0.016(\text{stat}) \pm 0.005(\text{syst})$ at 68% C.L. [23], excluding a zero value for θ_{13} with high significance. The same finding has been also reported by the RENO Collaboration [24], $\sin^2(2\theta_{13}) = 0.113 \pm 0.013(\text{stat}) \pm 0.019(\text{syst})$ (68% C.L.).

Finally, yet another important piece of information for reconstructing the neutrino asymmetries in the Universe is the measured value of the relativistic degrees of freedom in the early Universe, quantified in the so-called effective number of neutrinos, N_{eff}. In the case of the three active neutrino flavors with zero asymmetries and a standard thermal history, its value is the well-known $N_{\text{eff}} \simeq 3.046$ [25], but the presence of neutrino asymmetries can increase that number while still satisfying the BBN constraints [26]. Interestingly enough, recent CMB data has consistently given indications of N_{eff} higher than the standard value: recently the Atacama Cosmology Telescope (ACT) [27] and the South Pole Telescope (SPT) [28,29] have found

 © 2012 American Physical Society

evidence for $N_{\rm eff} > 3.046$ at 95% C.L., making the case for extra relativistic degrees of freedom stronger (see also [30]). It should however be kept in mind that other physical processes, like e.g. the contribution from the energy density of sterile neutrinos [31,32] or of gravitational waves [33], could also lead to a larger value for $N_{\rm eff}$.

Some recent papers have analyzed the impact of neutrino asymmetries with oscillations on BBN [26,34,35], mainly because data on light element abundances dominate the current limits on the asymmetries. Some studies using CMB data can be found in the literature (see for instance [36–38] for limits on the degeneracy parameters ξ_ν using the WMAP data and [39] for the effect of the primordial helium fraction in a Planck forecast), but our paper improves on that in two directions. First, we used for our analysis the neutrino spectra in the presence of asymmetries after taking into account the effect of flavor oscillations. Second, we checked the robustness of our results comparing the analysis of CMB and BBN data with a more complete set of cosmological data, including in particular supernovae Ia (SNIa) data [40], the measurement of the Hubble constant from the Hubble Space Telescope (HST) [41], and the Sloan Digital Sky Survey (SDSS) data on the matter power spectrum [42]. While current CMB measurements and the other data sets are not expected to improve significantly the constraints on the asymmetries, they constrain the sum of the neutrino masses, giving a more robust and general picture of the cosmological parameters.

Our goals in this work are twofold: first, we constrain the neutrino asymmetries and the sum of neutrino masses for both zero and nonzero values of θ_{13} using some of the latest cosmological data to obtain an updated and clear idea of the limits on them using current data; second, we perform a forecast of the constraints that could be achievable with future CMB experiments, taking as an example the proposed Cosmic Origins Explorer (COrE) [43] mission [44]. Given that current constraints are basically dominated by the BBN constraints, we use our forecast to answer the more general question of whether future CMB experiments can be competitive with the BBN bounds.

This paper is organized as follows. Initially, we briefly review in Sec. II the dynamics of the neutrino asymmetries prior to the BBN epoch. With those tools in hand, we proceed to study in Sec. III the impact on cosmological observables of the neutrino asymmetries for two values of the mixing angle θ_{13} using current cosmological data. We then step towards the future and describe in Sec. IV our forecast for the experiment COrE, where we study the potential of the future data from lensing of CMB anisotropies to constrain some of the cosmological parameters (in particular, neutrino asymmetries and the sum of the neutrino masses) with great precision. Finally, in Sec. V we draw our conclusions.

II. EVOLUTION OF COSMOLOGICAL NEUTRINOS WITH FLAVOR ASYMMETRIES

The dynamics of the neutrino distribution functions in the presence of flavor asymmetries and neutrino oscillations in the early Universe has been discussed in detail in the literature [26,34,35], and here we will only briefly review its main features and its consequences for the late cosmology.

We assume that flavor neutrino asymmetries, η_{ν_α}, were produced in the early Universe. At large temperatures frequent weak interactions keep neutrinos in equilibrium; thus, their energy spectrum follows a Fermi-Dirac distribution with a chemical potential μ_{ν_α} for each neutrino flavor. If $\xi_\alpha \equiv \mu_{\nu_\alpha}/T$ is the degeneracy parameter, the asymmetry is given by

$$\eta_{\nu_\alpha} \equiv \frac{n_{\nu_\alpha} - n_{\bar{\nu}_\alpha}}{n_\gamma} = \frac{1}{12\zeta(3)}[\pi^2\xi_\alpha + \xi_\alpha^3]. \tag{1}$$

Here n_{ν_α} ($n_{\bar{\nu}_\alpha}$) denotes the neutrino (antineutrino) number density, n_γ is the photon number density, and $\zeta(3) = 1.20206$.

As usual, we will write the radiation energy density of the Universe in terms of the parameter $N_{\rm eff}$, the effective number of neutrinos, as

$$\rho_r = \rho_\gamma\left[1 + \frac{7}{8}\left(\frac{4}{11}\right)^{4/3} N_{\rm eff}\right], \tag{2}$$

with $N_{\rm eff} = 3.046$ the value in the standard case with zero asymmetries and no extra relativistic degrees of freedom [25]. Assuming that equilibrium holds for the neutrino distribution functions, the presence of flavor asymmetries leads to an enhancement

$$\Delta N_{\rm eff} = \frac{15}{7}\sum_{\alpha=e,\mu,\tau}\left[2\left(\frac{\xi_\alpha}{\pi}\right)^2 + \left(\frac{\xi_\alpha}{\pi}\right)^4\right]. \tag{3}$$

Note that a neutrino degeneracy parameter of order $\xi_\alpha \gtrsim 0.3$ is needed in order to have a value of $\Delta N_{\rm eff}$ at least at the same level of the effect of nonthermal distortions discussed in [25]. This corresponds to $\eta_{\nu_\alpha} \sim \mathcal{O}(0.1)$. On the other hand, the primordial abundance of ^{4}He depends on the presence of an electron neutrino asymmetry and sets a stringent BBN bound on η_{ν_e} which does not apply to the other flavors, leaving a total neutrino asymmetry of order unity unconstrained [45,46]. However, this conclusion relies on the absence of effective neutrino oscillations that would modify the distribution of the asymmetries among the different flavors before BBN.

The evolution of the neutrino asymmetries in the epoch before BBN with three-flavor neutrino oscillations is found by solving the equations of motion for 3×3 density matrices of the flavor neutrinos as described in [47,48], including time-dependent vacuum and matter terms, both from background $e^\pm$ and neutrinos, as well as the collision integrals from neutrino weak interactions. This was done

under certain approximations in Refs. [15–17], where it was shown that neutrino oscillations are indeed effective before the onset of BBN. Therefore, the total lepton asymmetry is redistributed among the neutrino flavors and the BBN bound on η_{ν_e} can be translated into a limit on $\eta_\nu = \eta_{\nu_e} + \eta_{\nu_\mu} + \eta_{\nu_\tau}$, unchanged by oscillations and constant until electron-positron annihilations, when it decreases due to the increase in the photon number density.

The temperature at which flavor oscillations become effective is important not only to establish η_{ν_e} at the onset of BBN, but also to determine whether weak interactions with e^+e^- can still keep neutrinos in good thermal contact with the primeval plasma. Oscillations redistribute the asymmetries among the flavors, but only if they occur early enough that interactions would preserve Fermi-Dirac spectra for neutrinos, in such a way that the degeneracies ξ_α are well defined for each η_{ν_α} and the relation in Eq. (3) remains valid. This the case of early conversions of muon and tau neutrinos, since oscillations and collisions rapidly equilibrate their asymmetries at $T \simeq 15$ MeV [15]. Therefore one can assume the initial values $\eta^{\rm in}_{\nu_\mu} = \eta^{\rm in}_{\nu_\tau} \equiv \eta^{\rm in}_{\nu_x}$, leaving as free parameters $\eta^{\rm in}_{\nu_e}$ and the total asymmetry $\eta_\nu = \eta^{\rm in}_{\nu_e} + 2\eta^{\rm in}_{\nu_x}$.

If the initial values of the flavor asymmetries $\eta^{\rm in}_{\nu_e}$ and $\eta^{\rm in}_{\nu_x}$ have opposite signs, neutrino conversions will tend to reduce the asymmetries which in turn will decrease $N_{\rm eff}$. But if flavor oscillations take place at temperatures close to neutrino decoupling this would not hold and an extra contribution of neutrinos to radiation is expected with respect to the value in Eq. (3), as emphasized in [26] and shown in Fig. 1, where the $N_{\rm eff}$ isocontours for nonzero mixing are compared with those obtained from the frozen neutrino distributions taking into account the effect of flavor oscillations [34]. One can see that oscillations efficiently reduce $N_{\rm eff}$ for neutrino asymmetries with respect to the initial values from Eq. (3).

The evolution of the neutrino and antineutrino distribution functions with nonzero initial asymmetries, from $T = 10$ MeV until BBN, has been calculated in [26,34]. Here we use the final numerical results for these spectra in a range of values for $\eta^{\rm in}_{\nu_e}$ and η_ν as an input for our analysis, described in the next section. Note that an analysis in terms of the degeneracy parameters ξ_α as done for instance in [38] is no longer possible. We adopt the best-fit values for the neutrino oscillation parameters quoted in [18], assuming a normal hierarchy of the neutrino masses, except for the mixing angle θ_{13}, for which we will adopt two distinct values: $\theta_{13} = 0$ and $\sin^2\theta_{13} = 0.04$. The latter is close to the upper limit placed by the Daya Bay [23] and RENO [24] experiments on this mixing angle (with a best-fit value of $\sin^2\theta_{13} = 0.024$ and $\sin^2\theta_{13} = 0.029$, respectively), and is used as an example to understand the cosmological implications of a nonzero θ_{13}. Moreover, since the flavor asymmetries equilibrate for large values of this mixing angle, the cosmological effects are similar for $\sin^2\theta_{13} \gtrsim 0.02$, as in the case of an inverted hierarchy for a broad range of θ_{13} values (see, for instance, Fig. 4 of Ref. [35]). As for the case $\theta_{13} = 0$, though it seems presently disfavored with a high statistical significance after the Daya Bay and RENO results, we have decided to include it for comparison.

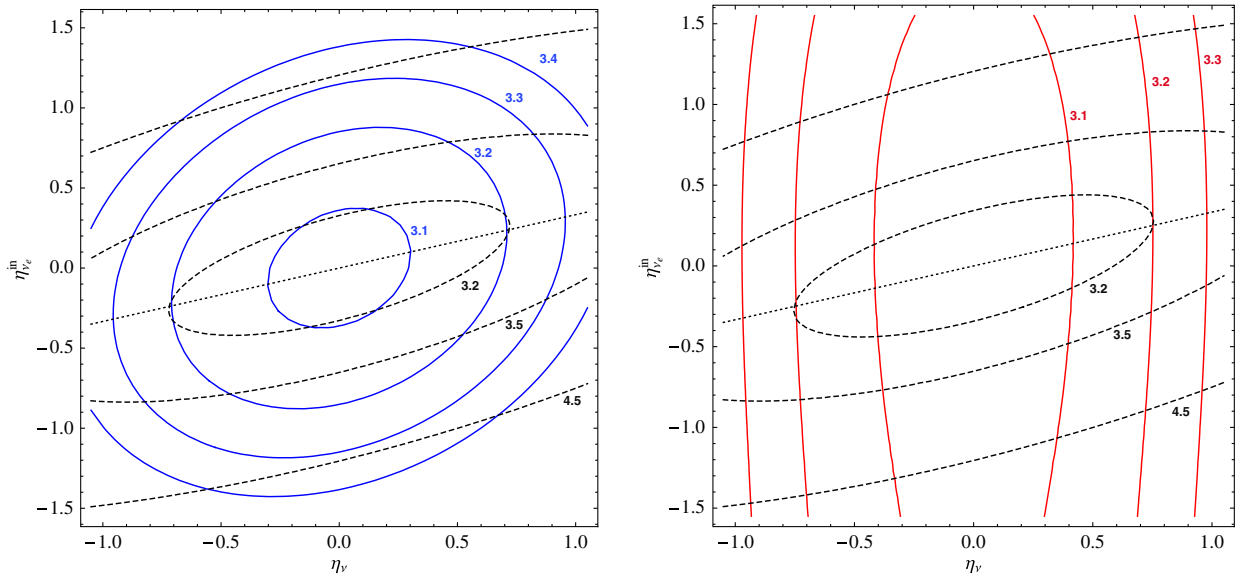

FIG. 1 (color online). Final contribution of neutrinos with primordial asymmetries to the radiation energy density. The isocontours of $N_{\rm eff}$ on the plane $\eta^{\rm in}_{\nu_e}$ vs η_ν, including flavor oscillations, are shown for two values of $\sin^2\theta_{13}$: 0 (blue solid curves, left panel) and 0.04 (red solid curves, right panel) and compared to the case with zero mixing (dashed curves). The dotted line corresponds to $\eta_\nu = \eta_{\nu_x}$ ($x = \mu, \tau$), where one expects oscillations to have negligible effects.

TABLE I. Cosmological and neutrino parameters.

Type	Symbol	Meaning	Uniform prior
Primary	$\Omega_b h^2$	Baryon density	(0.005, 0.1)
Cosmological	$\Omega_{dm} h^2$	Dark matter density[a]	(0.01, 0.99)
Parameters	τ	Optical depth to reionization	(0.01, 0.8)
	$100\theta_s$	Angular scale of the sound horizon at the last scattering	(0.5, 10)
	n_s	Scalar index of the power spectrum	(0.5, 1.5)
	$\log[10^{10} A_s]$	Scalar amplitude of the power spectrum [b]	(2.7, 4)
Neutrino	m_1(eV)	Mass of the lightest neutrino [c]	(0, 1)
Parameters	η_ν	Total asymmetry at $T = 10$ MeV	$(-0.8, 0.8)$
	$\eta^{\rm in}_{\nu_e}$	Initial electron neutrino asymmetry at $T = 10$ MeV	$(-1.2, 1.2)$
Derived	h	Reduced Hubble constant[d]	···
Parameters	$\Delta N_{\rm eff}$	Enhancement to the standard effective number of neutrinos[e]	···

[a]Also includes neutrinos.
[b]at the pivot wavenumber $k_0 = 0.05\ {\rm Mpc}^{-1}$.
[c]We assume here normal hierarchy.
[d]$H_0 = 100h\ {\rm km\,s^{-1}\,Mpc^{-1}}$.
[e]$N_{\rm eff} = 3.046$.

III. COSMOLOGICAL CONSTRAINTS ON NEUTRINO PARAMETERS

Having set the basic framework for the calculation of the neutrino distribution functions in the presence of asymmetries and for different θ_{13}, we can now proceed to investigate its cosmological effects.

In order to constrain the values of the cosmological neutrino asymmetries, we compare our results to the observational data. In particular, we use a modified version of the CAMB code [49] to evolve the cosmological perturbations and obtain the CMB and matter power spectra in the presence of nonzero neutrino asymmetries in the neutrino distribution functions. We checked that the spectra computed by our modified CAMB version are consistent up to high accuracy with those obtained with CLASS [50], that incorporates the models considered here in its public version. This version of CAMB is interfaced with the Markov chain Monte Carlo package CosmoMC [51] that we use to sample the parameter space and obtain the posterior distributions for the parameters of interest.

We derive our constraints in the framework of a flat ΛCDM model with the three standard model neutrinos and purely adiabatic initial conditions. The parameters we use are described in Table I as well as the range of the flat priors used. As can be seen, six of them are the standard ΛCDM cosmological parameters, and we add to those three new parameters, namely the mass of the lightest neutrino mass eigenstate m_1 (the other two masses are calculated using the best fit for Δm^2_{21} and Δm^2_{31} obtained in [18], assuming normal hierarchy) and the two neutrino asymmetries we mentioned earlier, $\eta^{\rm in}_{\nu_e}$ and η_ν. The values of the effective degeneracy parameters ξ_α after BBN,[1] needed by CAMB, are precalculated as a function of the asymmetries (following the method described in the previous section) over a grid in $(\eta^{\rm in}_{\nu_e}, \eta_\nu)$ and stored on a table, used for interpolation during the Monte Carlo run.

A comment on the parametrization is in order. It is a standard practice in cosmological analyses to parametrize the neutrino masses via $\Omega_\nu h^2$ or equivalently $f_\nu \equiv \Omega_\nu/\Omega_{dm}$, and from that (assuming that neutrinos decoupled at equilibrium) derive the sum of neutrino masses, which are taken to be degenerate. The presence of lepton asymmetries dramatically changes this simple scheme. Now the neutrino number density is a complicated function of the η's obtained from a nonequilibrium distribution function. When f_ν is used, any effect related to the way in which the total neutrino density is shared among the different mass eigenstates is completely lost. In that sense, the parametrization used in this paper looks more physically motivated since energy densities of neutrinos are constructed from two fundamental quantities, namely their phase space distributions and their masses.

The most basic data set that we consider only consists of the WMAP 7-year temperature and polarization anisotropy data. We will refer to it simply as "WMAP." The likelihood is computed using the the WMAP likelihood code publicly available at the LAMBDA website [52]. We marginalize over the amplitude of the Sunyaev-Zel'dovich signal.

[1]The neutrino distribution functions can be parametrized by Fermi-Dirac-like functions with an effective ξ_α and temperature T_α [34], which are related to the first two moments of the distribution, the number density and energy density.

In addition to the WMAP data, we also include the BBN measurement of the ^{4}He mass fraction Y_p from the data collection analysis done in [53], in the form of a Gaussian prior

$$Y_p = 0.250 \pm 0.003(1\sigma). \quad (4)$$

Indeed, some authors have recently reported a larger central value, $Y_p \sim 0.257$ [54–56], with quite different uncertainty determinations. In [57] using a Markov chain Monte Carlo technique already exploited in [56], the primordial value of ^{4}He decreased again to $Y_p = 0.2534 \pm 0.0083$, which is compatible at 1σ with (4). We will not use these results in our analysis, but we will comment on their possible impact in the following. We also note that in [58] a robust upper bound $Y_p < 0.2631$ (95% C.L.) has been derived based on very weak assumptions on the astrophysical determination of ^{4}He abundance, namely that the minimum effect of star processing is to keep constant the helium content of a low-metallicity gas, rather than increase it, as expected. As we will show, the measurement of Y_p currently dominates the constraints on the asymmetries: if we were to conservatively allow for larger uncertainties on that measurement, like for example those reported in [57], our constraints from present data would correspondingly be weakened. Moreover, we decided not to use the deuterium measurements since at the moment they are not competitive with helium for constraining the asymmetries (see, e.g., Fig. 6 of Ref. [34]), although there are recent claims that they could place strong constraints on $N_{\rm eff}$ at the level of $\Delta N_{\rm eff} \simeq \pm 0.5$ [59]. This is a very interesting perspective but at the moment, deuterium measurements in different QSO absorption line systems show a significant dispersion, much larger than the quoted errors.

The data set that uses both WMAP 7-year data and the determination of the primordial abundance of helium as in (4) will be referred to as "WMAP + He." Measurements of Y_p represent the best "leptometer" currently available, in the sense that they place the most stringent constraints on lepton asymmetries for a given baryonic density [60]. The ^{4}He mass fraction depends on the baryonic density, the electron neutrino degeneracy parameter and the effective number of neutrino families. Thus, in order to consistently implement the above determination of Y_p in our Monte Carlo analysis, we compute $\Delta N_{\rm eff}$ and ξ_e coming from the distribution functions calculated with the asymmetries (as explained in the previous section) and store them on a table. During the CosmoMC run, we use this table to obtain by interpolation the values $\Delta N_{\rm eff}$ and ξ_e corresponding to given values of the asymmetries (which are the parameters actually used in the Monte Carlo), and finally to obtain Y_p as a function of $\Delta N_{\rm eff}$, ξ_e and $\Omega_b h^2$. Notice that this approach is slightly less precise than the one used in Refs. [34,35], where a full BBN analysis was performed, but this approximation should suffice for our purposes, especially taking into account that we will be comparing BBN limits on the asymmetries with the ones placed by other cosmological data, that as we shall see are far less constraining. In any case, we have checked that the agreement between the interpolation scheme and the full BBN analysis is at the percent level.

We derive our constraints from parallel chains generated using the Metropolis-Hastings algorithm. For a subset of the models, we have also generated chains using the slice sampling method, in order to test the robustness of our results against a change in the algorithm. We use the

TABLE II. 95% C.L. constraints on cosmological parameters for the WMAP and WMAP + He data sets.

Parameter	WMAP $\sin^2\theta_{13} = 0$	$\sin^2\theta_{13} = 0.04$	WMAP + He $\sin^2\theta_{13} = 0$	$\sin^2\theta_{13} = 0.04$
$100\Omega_b h^2$	$2.20^{+0.14}_{-0.12}$	$2.20^{+0.13}_{-0.12}$	2.20 ± 0.12	2.20 ± 0.12
$\Omega_{dm} h^2$	0.118 ± 0.016	$0.117^{+0.017}_{-0.016}$	0.119 ± 0.017	0.117 ± 0.016
τ	$0.085^{+0.029}_{-0.026}$	$0.085^{+0.030}_{-0.027}$	$0.085^{+0.030}_{-0.027}$	$0.085^{+0.029}_{-0.027}$
$100\theta_s$	1.0387 ± 0.0063	$1.0389^{+0.0069}_{-0.0063}$	$1.0381^{+0.054}_{-0.053}$	$1.0387^{+0.0053}_{-0.0054}$
n_s	0.953 ± 0.032	$0.953^{+0.032}_{-0.033}$	$0.955^{+0.034}_{-0.035}$	$0.952^{+0.031}_{-0.032}$
$\log[10^{10}A_s]$	$3.064^{+0.080}_{-0.082}$	$3.062^{+0.080}_{-0.079}$	$3.068^{+0.081}_{-0.078}$	$3.062^{+0.073}_{-0.075}$
m_1 (eV)	≤ 0.39	≤ 0.38	≤ 0.38	≤ 0.38
$\eta^{\rm in}_{\nu_e}$	...[a]	...[a]	...[a]	...[a]
η_ν	...[a]	...[a]	$[-0.64; 0.72]$	$[-0.071; 0.054]$
h	$0.652^{+0.084}_{-0.083}$	$0.653^{+0.081}_{-0.082}$	$0.656^{+0.084}_{-0.081}$	$0.650^{+0.078}_{-0.081}$
$\Delta N_{\rm eff}$	≤ 0.32	≤ 0.16	≤ 0.43	≤ 0.03

[a]The 95% confidence region is not well-defined in these cases because the posterior does not vanish at the end of the prior range (see e.g. the middle panel of Fig. 2). See discussion in the text.

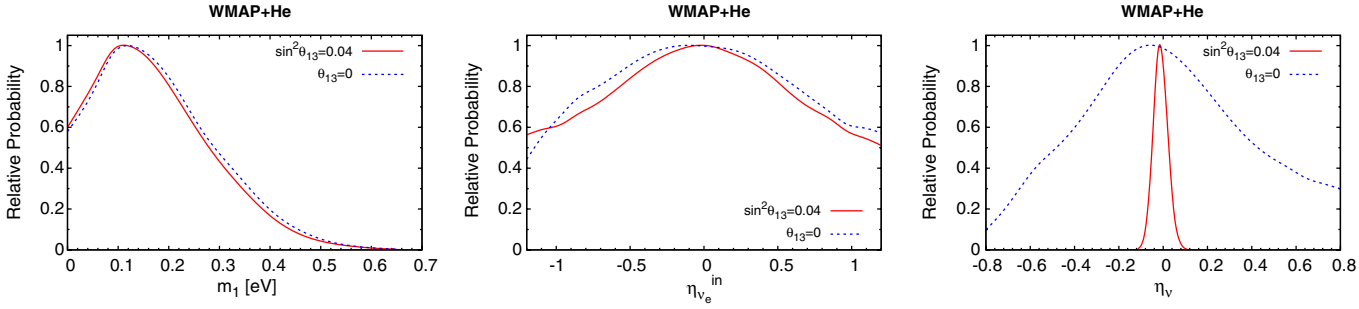

FIG. 2 (color online). One-dimensional posterior probability density for m_1, $\eta_{\nu_e}^{\rm in}$, and η_ν for the WMAP + He data set.

Gelman and Rubin R parameter to evaluate the convergence of the chains, demanding that $R - 1 < 0.03$. The one- and two-dimensional posteriors are derived by marginalizing over the other parameters.

Our results for the cosmological and neutrino parameters from the analysis are shown in Table II, while Fig. 2 shows the marginalized one-dimensional probability distributions for the lightest neutrino mass, the initial electron-neutrino asymmetry, and the total asymmetry, for the different values of θ_{13}. Notice that the posterior for $\eta_{\nu_e}^{\rm in}$ (middle panel) is still quite large at the edges of the prior range. This happens also for both the $\eta_{\nu_e}^{\rm in}$ and η_ν posteriors obtained using only the WMAP data (not shown in the figure). Since the priors on these parameters do not represent a real physical constraint (as in the case $m_\nu > 0$), but just a choice of the range to explore, we refrain from quoting 95% credible intervals in these cases, as in order to do this one would need knowledge of the posterior in all the regions where it significantly differs from zero. However, it is certain that the *actual* 95% C.I. includes the one that one would obtain using just part of the posterior (as long as this contains the peak of the distribution). If we do this, we obtain constraints that are anyway much worse than those from BBN. Finally, we also stress that if a larger experimental determination of Y_p or measurements with larger uncertainties were used, as those reported in [54–56], BBN would show a preference for larger values of $N_{\rm eff}$ as well.

Concerning the neutrino asymmetries, shown in the middle and right panels of Fig. 2, we notice that while the initial flavor asymmetries remain highly unconstrained by current data, the total asymmetry constraint improves significantly for $\theta_{13} \neq 0$. This result agrees with previous results from BBN-only studies [34,35], and it is a result of the equilibration of flavor asymmetries when θ_{13} is large (see, e.g., Fig. 5 of Ref. [34]). When the flavors equilibrate in the presence of a nonzero mixing angle ($\sin^2\theta_{13} = 0.04$ in our example) the total asymmetry is distributed almost equally among the different flavors, leading to a final asymmetry $\eta_{\nu_e}^{\rm fin} \approx \eta_{\nu_x}^{\rm fin} \approx \eta_\nu/3$ (where $x = \mu, \tau$). Hence, the fact that the BBN prior requires $\eta_{\nu_e}^{\rm fin} \approx 0$ for the correct abundance of primordial helium (see Fig. 3) leads to a strong constraint on the constant total asymmetry, $-0.071 \leq \eta_\nu \leq 0.054$ (95% C.L.).

On the other hand, since the constraints come most from the distortion in the electron neutrino distribution function, when $\theta_{13} = 0$ (and therefore there is less mixing) the direct relation between $\eta_{\nu_e}^{\rm fin}$ and η_ν is lost. In this case, the total asymmetry could still be large, even if the final electron neutrino asymmetry is small, as significantly asymmetries can still be stored on the other two flavors, leading to a constraint an order of magnitude weaker than the previous case, $-0.64 \leq \eta_\nu \leq 0.72$ (95% C.L.). As expected, this is reflected on the allowed ranges for $\Delta N_{\rm eff}$, as shown in Fig. 4: while for $\theta_{13} = 0$ the $\Delta N_{\rm eff} \simeq 0.5$ are still allowed by the data, nonzero values of this mixing angle reduce the allowed region in the parameter space by approximately an order of magnitude in both $\Delta N_{\rm eff}$ and η_ν.

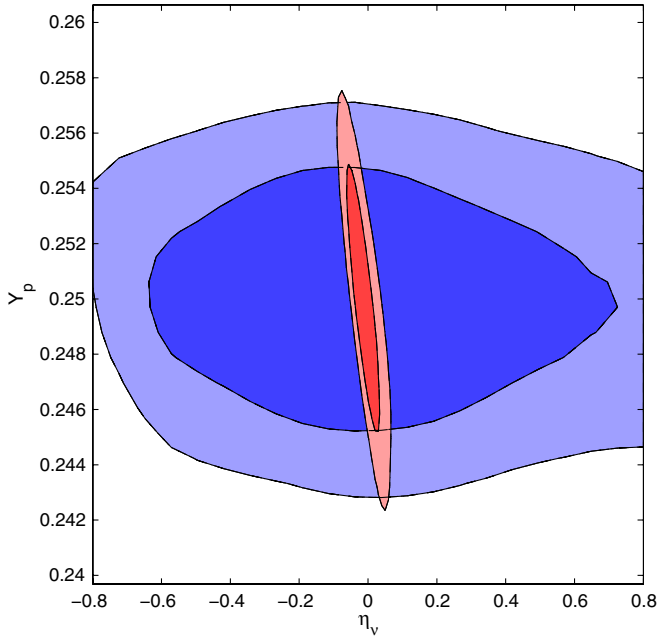

FIG. 3 (color online). 68% and 95% confidence regions in total neutrino asymmetry η_ν vs the primordial abundance of helium Y_p plane for $\theta_{13} = 0$ (larger blue contours) and $\sin^2\theta_{13} = 0.04$ (smaller red contours), from the analysis of the WMAP + He data set. Notice the much stronger constraint for the nonzero mixing angle due to the faster equilibration of flavor asymmetries.

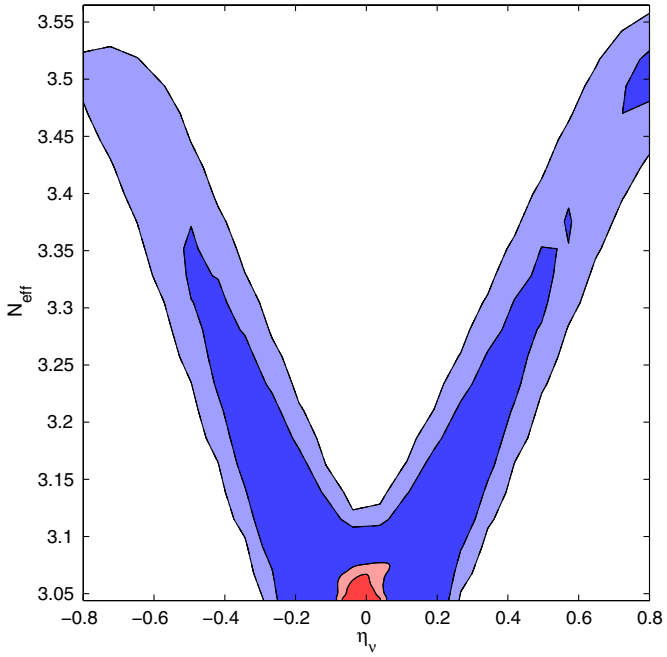

FIG. 4 (color online). Two-dimensional 68% and 95% confidence regions in the $(\eta_\nu, N_{\rm eff})$ plane from the analysis of the WMAP + He data set, for $\theta_{13} = 0$ (larger blue contours) and $\sin^2\theta_{13} = 0.04$ (smaller red contours). Even for zero θ_{13} the data seem to favor $N_{\rm eff}$ around the standard value $N_{\rm eff} = 3.046$.

We confirmed in our analysis that the constraints on the asymmetry are largely dominated by the BBN prior at present. This is shown in Fig. 5, where we compare the results of our analysis with a more complete data set (which we refer to as ALL) that includes distance measurements of SNIa from the SDSS compilation [40] and the HST determination of the Hubble constant H_0 [41], as well as data on the power spectrum of the matter density field, as reconstructed from a sample of luminous red galaxies of the SDSS Seventh Data Release [42]. This is due to the fact that other cosmological data constrain the asymmetries via their effect on increasing $N_{\rm eff}$, and currently the errors on the measurement of the effective number of neutrinos [1,27–29] are significantly weaker than our prior on Y_p, Eq. (4).[2] The fact that bounds on leptonic asymmetries are dominated by the BBN prior (i.e. by ^{4}He data) is also confirmed by the similarity of our bounds on $(\eta_\nu, \eta^{\rm in}_{\nu_e})$ with those of [35]. Note that the limits reported in [35] sound weaker, because they are frequentist bounds obtained by cutting the parameter probability at $\Delta\chi^2 = 6.18$, i.e. they represent 95% bounds on joint two-dimensional parameter probabilities (in the Gaussian approximation). The one-dimensional 95% confidence limits,

[2]On the other hand, these other cosmological data sets have an impact on other parameters like e.g. the neutrino mass. But since in this work we are primarily interested in bounding the asymmetries, we prefer to stick to the robust WMAP + He data set. In that way, our results are not contaminated by possible systematic uncertainties in the other data. Actually, the inclusion of all external data sets (in particular, of SNIa together with H_0) reveals a conflict between them, leading to a bimodal posterior probability for $\Omega_{dm}h^2$ and to a preference for $m_1 > 0$ at 95% C.L.

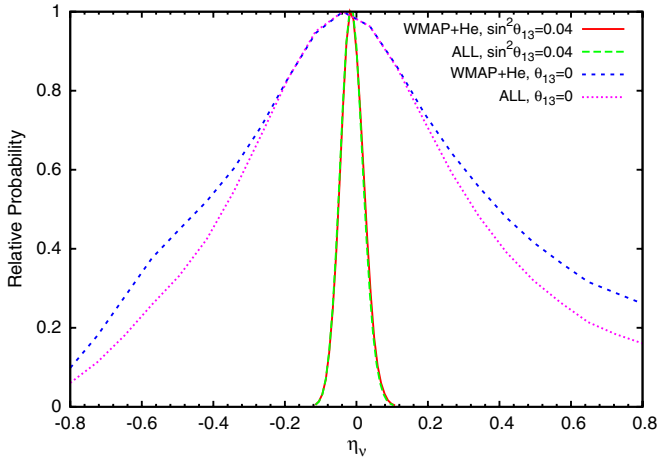

FIG. 5 (color online). One-dimensional posterior probability density for η_ν comparing the WMAP + He and the ALL data sets. As mentioned in the text, the constraints on the total asymmetry do not improve significantly with the inclusion of other cosmological data sets, as they are mainly driven by the determination of the primordial helium abundance.

TABLE III. Experimental specifications for COrE [44]. For each channel, we list the channel frequency in GHz, the FWHM in arcminutes, the temperature (σ_T) and polarization (σ_P) noise per pixel in μK.

Frequency [GHz]	$\theta_{\rm fwhm}$ [arcmin]	σ_T [μK]	σ_P [μK]
105	10.0	0.268	0.463
135	7.8	0.337	0.583
165	6.4	0.417	0.720
195	5.4	0.487	0.841
225	4.7	0.562	0.972

TABLE IV. Fiducial values for the cosmological parameters for the COrE forecast.

Parameter	Fiducial value ($\sin^2\theta_{13} = 0$)	Fiducial value ($\sin^2\theta_{13} = 0.04$)
$\Omega_b h^2$	0.0218	0.0224
$\Omega_{dm} h^2$	0.121	0.118
τ	0.0873	0.0865
h	0.709	0.705
n_s	0.978	0.968
$\log[10^{10} A_s]$	3.12	3.08
m_1 (eV)	0.02	0.02
$\eta^{\rm in}_{\nu_e}$	0	0
η_ν	0	0

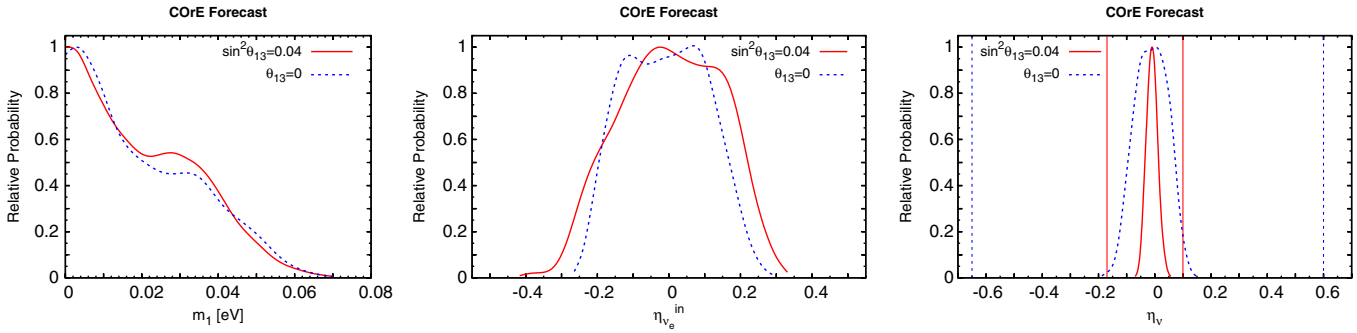

FIG. 6 (color online). One-dimensional probability distribution function for m_1 and η_ν for COrE forecast. The middle panel shows that an experiment like COrE could start to constrain the initial electron neutrino asymmetry. The vertical lines on the right panel show the current 95% C.L. obtained in the previous section. The errors on the asymmetries are improved by approximately a factor 6.6 or 1.6 for $\theta_{13} = 0$ and $\sin^2\theta_{13} = 0.04$, respectively, compared to the results shown in Fig. 2.

corresponding to $\Delta\chi^2 = 4$, are smaller and very close to the results of the present paper. We also checked that using our codes and data sets, we obtain very similar results when switching from Bayesian to frequentist confidence limits.

We conclude this section noting that the current constraints on the sum of neutrino masses are robust under a scenario with lepton asymmetries, as those extra degrees of freedom do not correlate with the neutrino mass. On the other hand, to go beyond the BBN limits on the asymmetries more precise measurements of $N_{\rm eff}$ are clearly needed, and in the next section we forecast the results that could be achievable with such an improvement using COrE as an example of future CMB experiments.

IV. FORECAST

Given that the current constraints on the lepton asymmetries are dominated by their effect on the primordial production of light elements, one can ask whether future cosmological experiments can improve over the current limits imposed by BBN. With that goal in mind, we take as an example a proposed CMB experiment, COrE (Cosmic Origins Explorer) [44], designed to detect the primordial gravitational waves and measure the CMB gravitational lensing deflection power spectrum on all linear scales to the cosmic variance limit. The latter is of special interest for this work, as the CMB lensing is expected to probe with high sensitivity the absolute neutrino masses and $N_{\rm eff}$ [61].

We used the package FuturCMB [62] in combination with CAMB and CosmoMC for producing mock CMB data, and fit it with a likelihood based on the potential sensitivity of COrE. We include, also in this case, the information coming from present measurements of the helium fraction, encoded in the Gaussian prior (4). We consider five of COrE's frequency channels, ranging from 105 to 225 GHz, with the specifications given in [44] and reported for convenience in Table III, and assume an observed fraction $f_{\rm sky} = 0.65$. We do not consider other channels as they are likely to be foreground dominated. We take a maximum multipole $\ell_{\rm max} = 2500$. In our analysis, we have assumed that the uncertainties associated to the beam and foregrounds have been properly modeled and removed, so that we can only consider the statistical uncertainties. Those are optimistic assumptions, as under realistic conditions systematic uncertainties will certainly play an important role. In that sense, our results represent an illustration of what future CMB experiments could ideally achieve.

We use CMB lensing information in the way described in [63], assuming that the CMB lensing potential spectrum will be extracted from COrE maps with a quadratic estimator technique.

For the forecast we adopt the fiducial values for the cosmological parameters shown in Table IV for both cases of θ_{13} discussed previously. The two sets of fiducial values correspond to the best-fit models of the WMAP + He data set for the two values of θ_{13}. In the case of the neutrino mass, since the likelihood is essentially flat between 0 and 0.2 eV, we have chosen to take $m_1 = 0.02$ eV. This is below the expected sensitivity of COrE and should thus be essentially equivalent to the case where the lightest neutrino is massless.

The sensitivities on the neutrino parameters for COrE are shown in Fig. 6 for the two values of θ_{13}. As expected for the sum of the neutrino masses, the constraints are significantly better than the current ones, and could in principle start probing the minimal values guaranteed by flavor oscillations [61]. Note that our forecast error for m_1 differs slightly from the one presented in [44], most probably because the forecasts in

TABLE V. 95% confidence intervals for the neutrino parameters with COrE.

Parameter	$\sin^2\theta_{13} = 0$	$\sin^2\theta_{13} = 0.04$
m_1 (eV)	<0.049	<0.048
$\eta_{\nu_e}^{\rm in}$	$[-0.20; 0.20]$	$[-0.25; 0.24]$
η_ν	$[-0.12; 0.09]$	$[-0.048; 0.030]$

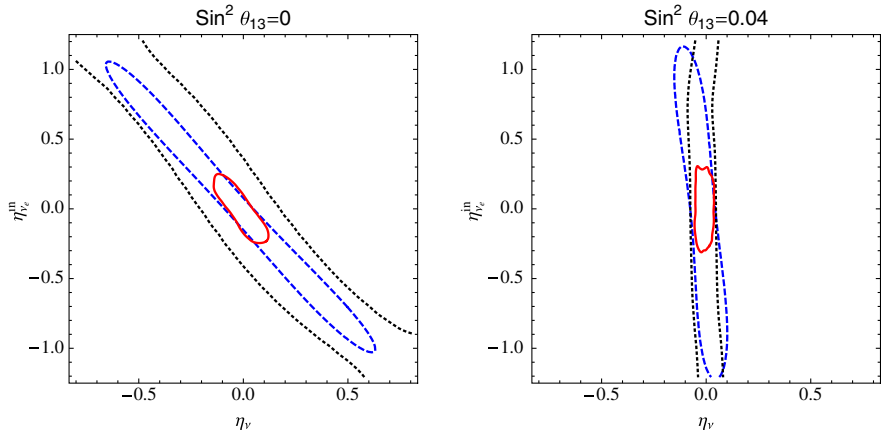

FIG. 7 (color online). The 95% C.L. contours on the η_ν vs $\eta_{\nu_e}^{\rm in}$ plane from our analysis with current data (WMAP + He data set, black dotted) compared to the results of the BBN analysis of Ref. [35] (blue dashed) and with the COrE forecast (red solid).

this reference are based on the Fisher matrix approximation. But our main goal in this section is to discuss how COrE observations will help improve the limits on the asymmetries discussed previously, that are basically dominated by the available measurements of the ^{4}He abundance. The right panel of Fig. 6 shows the forecasted posterior probability distribution for η_ν, and the marginalized constraints for it are listed in Table V for both values of θ_{13}; in particular, the vertical lines of the right panel show the 95% C.L. limits obtained from the full BBN analysis of Ref. [35]. Comparing the values from Tables II and V one can see that an experiment like COrE would improve current 95% limits on the total leptonic asymmetry by nearly factors 6.6 ($\theta_{13} = 0$) and 1.6 ($\sin^2\theta_{13} = 0.04$), competitive over the constraints from ^{4}He abundance only. It should be noted that the error bars on the primordial abundances are very difficult to reduce due to systematic errors on astrophysical measurements [53], and therefore it is feasible that CMB experiments will be an important tool in the future to improve the constraints on the asymmetries. Notice however that, since the CMB is insensitive to the sign of the η's, BBN measurements will still be needed in order to break this degeneracy.

Finally, in Fig. 7 we show the COrE sensitivity on the asymmetries in the plane η_ν vs $\eta_{\nu_e}^{\rm in}$ compared to the constraints of Sec. III obtained using current data and to the full BBN analysis of Ref. [35]. Notice that in the case $\theta_{13} = 0$ the constraints of the previous section are quite less constraining than the ones coming from the full BBN analysis because we are not using deuterium data, known to be important to close the contours on the asymmetries plane, especially for small values of θ_{13} [34]. Moreover, future CMB experiments have the potential to reduce the allowed region, dominating the errors in this analysis.

In summary, an experiment like COrE is capable of improving the constraints on the lepton asymmetries by up to a factor 6.6 on the total and/or flavor asymmetries depending on the value of the mixing angle θ_{13}. In addition to that, such an experiment would also constrain other cosmological parameters (in particular the sum of the neutrino masses) with significant precision, providing yet another step towards the goal of accurately measuring the properties of the Universe.

V. CONCLUSIONS

Understanding the physical processes that took place in the early Universe is a crucial ingredient for deciphering the physics at energies that cannot be currently probed in terrestrial laboratories. In particular, since the origin of the matter-antimatter is still an open question in cosmology, it is important to keep an open mind for theories that predict large lepton asymmetries. In that case, constraining total and flavor neutrino asymmetries using cosmological data is a way to test and constrain some of the possible particle physics scenarios at epochs earlier than the BBN.

For that, we initially used current cosmological data to constrain not only the asymmetries, but also to understand the robustness of the cosmological parameters (and the limits on the sum of the neutrino masses) for two different values of the mixing angle θ_{13} to account for the evidences of a nonzero value for this angle. Our results confirm the fact that at present the limits on the cosmological lepton asymmetries are dominated by the abundance of primordial elements generated during the BBN, in particular the abundance of ^{4}He, currently the most sensitive "leptometer" available.

However, future CMB experiments might be able to compete with BBN data in what concerns constraining lepton asymmetries, although BBN will always be needed in order to get information on the sign of the η's. We took as an example the future CMB mission COrE, proposed to measure with unprecedented precision the lensing of CMB anisotropies, and our results indicate that it has the potential to significantly improve over current constraints while, at the

same time placing limits on the sum of the neutrino masses that are of the order of the neutrino mass differences.

Finally, we notice that for the values of θ_{13} measured by the Daya Bay and RENO experiments the limits on the cosmological lepton asymmetries and on its associated effective number of neutrinos are quite strong, so that lepton asymmetries cannot increase $N_{\rm eff}$ significantly above 3.4. Under those circumstances, if the cosmological data (other than BBN) continues to push for large values of $N_{\rm eff}$, new pieces of physics such as sterile neutrinos will be necessary to explain that excess.

ACKNOWLEDGMENTS

We thank Srdjan Sarikas for providing some of the data used in Figs. 1 and 7. The work of A. M. was supported by the PRIN-INAF grant "Astronomy Probes Fundamental Physics" and by the Italian Space Agency through the ASI contract Euclid- IC (I/031/10/0). G. M. acknowledges support by the *Instituto Nazionale di Fisica Nucleare* I.S. FA51 and the PRIN 2010 "Fisica Astroparticellare: Neutrini ed Universo Primordiale" of the Italian *Ministero dell'Istruzione, Università e Ricerca*. The work of M. L. is supported by Ministero dell'Istruzione, dell'Universit e della Ricerca (MIUR) through the PRIN grant "Matter-Antimatter Asymmetry, Dark Matter and Dark Energy in the LHC Era" (Contract No. PRIN 2008NR3EBK-005). S. P. and U. F. were supported by the Spanish grants FPA2008-00319, FPA2011-22975 and Multidark CSD2009-00064 (MINECO) and PROMETEO/2009/091 (Generalitat Valenciana), and by the EC contract UNILHC PITN-GA-2009-237920. U. F. acknowledges the support of the I3P-CSIC and of EPLANET. This research was also supported by a Spanish-Italian MINECO-INFN agreement, refs. AIC10-D-000543 and AIC-D-2011-0689. Finally, E. C. acknowledges the hospitality of CERN while working on this paper.

[1] E. Komatsu *et al.* (WMAP Collaboration), Astrophys. J. Suppl. Ser. **192**, 18 (2011).
[2] A. Casas, W. Y. Cheng, and G. Gelmini, Nucl. Phys. **B538**, 297 (1999).
[3] J. March-Russell, H. Murayama, and A. Riotto, J. High Energy Phys. 11 (1999) 015.
[4] J. McDonald, Phys. Rev. Lett. **84**, 4798 (2000).
[5] D. J. Schwarz and M. Stuke, J. Cosmol. Astropart. Phys. 11 (2009) 025.
[6] V. B. Semikoz, D. D. Sokoloff, and J. W. F. Valle, Phys. Rev. D **80**, 083510 (2009).
[7] X.-D. Shi and G. M. Fuller, Phys. Rev. Lett. **82**, 2832 (1999).
[8] M. Laine and M. Shaposhnikov, J. Cosmol. Astropart. Phys. 06 (2008) 031.
[9] M. Stuke, D. J. Schwarz, and G. Starkman, J. Cosmol. Astropart. Phys. 03 (2012) 040.
[10] D. H. Lyth, C. Ungarelli, and D. Wands, Phys. Rev. D **67**, 023503 (2003).
[11] C. Gordon and K. A. Malik, Phys. Rev. D **69**, 063508 (2004).
[12] E. Di Valentino, M. Lattanzi, G. Mangano, A. Melchiorri, and P. Serpico, Phys. Rev. D **85**, 043511 (2012).
[13] J. Lesgourgues and S. Pastor, Phys. Rev. D **60**, 103521 (1999).
[14] J. Lesgourgues and S. Pastor, Phys. Rep. **429**, 307 (2006).
[15] A. D. Dolgov, S. H. Hansen, S. Pastor, S. T. Petcov, G. G. Raffelt, and D. V. Semikoz, Nucl. Phys. **B632**, 363 (2002).
[16] Y. Y. Y. Wong, Phys. Rev. D **66**, 025015 (2002).
[17] K. N. Abazajian, J. F. Beacom, and N. F. Bell, Phys. Rev. D **66**, 013008 (2002).
[18] T. Schwetz, M. Tortola, and J. W. F. Valle, New J. Phys. **13**, 063 004 (2011).
[19] G. L. Fogli, E. Lisi, A. Marrone, A. Palazzo, and A. M. Rotunno, Phys. Rev. D **84**, 053007 (2011).
[20] K. Abe *et al.* (T2K Collaboration), Phys. Rev. Lett. **107**, 041801 (2011).
[21] P. Adamson *et al.* (MINOS Collaboration), Phys. Rev. Lett. **107**, 181802 (2011).
[22] Y. Abe *et al.* (DOUBLE-CHOOZ Collaboration), Phys. Rev. Lett. **108**, 131801 (2012).
[23] F. P. An *et al.* (DAYA-BAY Collaboration), Phys. Rev. Lett. **108**, 171803 (2012).
[24] J. K. Ahn *et al.* (RENO Collaboration), Phys. Rev. Lett. **108**, 191802 (2012).
[25] G. Mangano, G. Miele, S. Pastor, T. Pinto, O. Pisanti, and P. D. Serpico, Nucl. Phys. **B729**, 221 (2005).
[26] S. Pastor, T. Pinto, and G. G. Raffelt, Phys. Rev. Lett. **102**, 241302 (2009).
[27] J. Dunkley *et al.* (ACT Collaboration), Astrophys. J. **739**, 52 (2011).
[28] R. Keisler *et al.* (SPT Collaboration), Astrophys. J. **743**, 28 (2011).
[29] B. A. Benson *et al.* (SPT Collaboration), arXiv:1112.5435.
[30] M. Archidiacono, E. Calabrese, and A. Melchiorri, Phys. Rev. D **84**, 123008 (2011).
[31] E. Giusarma, M. Corsi, M. Archidiacono, R. de Putter, A. Melchiorri, O. Mena, and S. Pandolfi, Phys. Rev. D **83**, 115023 (2011).
[32] J. Hamann, S. Hannestad, G. G. Raffelt, and Y. Y. Y. Wong, J. Cosmol. Astropart. Phys. 09 (2011) 034.
[33] I. Sendra and T. L. Smith, Phys. Rev. D **85**, 123002 (2012).
[34] G. Mangano, G. Miele, S. Pastor, O. Pisanti, and S. Sarikas, J. Cosmol. Astropart. Phys. 03 (2011) 035.
[35] G. Mangano, G. Miele, S. Pastor, O. Pisanti, and S. Sarikas, Phys. Lett. B **708**, 1 (2012).
[36] M. Lattanzi, R. Ruffini, and G. V. Vereshchagin, Phys. Rev. D **72**, 063003 (2005).
[37] L. A. Popa and A. Vasile, J. Cosmol. Astropart. Phys. 06 (2008) 028.

[38] M. Shiraishi, K. Ichikawa, K. Ichiki, N. Sugiyama, and M. Yamaguchi, J. Cosmol. Astropart. Phys. 07 (2009) 005.
[39] J. Hamann, J. Lesgourgues, and G. Mangano, J. Cosmol. Astropart. Phys. 03 (2008) 004.
[40] R. Kessler *et al.*, Astrophys. J. Suppl. Ser. **185**, 32 (2009).
[41] A. G. Riess *et al.*, Astrophys. J. **699**, 539 (2009).
[42] B. A. Reid *et al.*, Mon. Not. R. Astron. Soc. **404**, 60 (2010).
[43] http://www.core-mission.org.
[44] F. R. Bouchet *et al.* (The COrE Collaboration), arXiv:1102.2181.
[45] H. S. Kang and G. Steigman, Nucl. Phys. **B372**, 494 (1992).
[46] S. H. Hansen, G. Mangano, A. Melchiorri, G. Miele, and O. Pisanti, Phys. Rev. D **65**, 023511 (2001).
[47] G. Sigl and G. Raffelt, Nucl. Phys. **B406**, 423 (1993).
[48] B. H. J. McKellar and M. J. Thomson, Phys. Rev. D **49**, 2710 (1994).
[49] A. Lewis, A. Challinor, and A. Lasenby, Astrophys. J. **538**, 473 (2000); http://camb.info/.
[50] D. Blas, J. Lesgourgues, and T. Tram, J. Cosmol. Astropart. Phys. 07 (2011) 034.
[51] A. Lewis and S. Bridle, Phys. Rev. D **66**, 103511 (2002); http://cosmologist.info/cosmomc/.
[52] http://lambda.gsfc.nasa.gov/.
[53] F. Iocco, G. Mangano, G. Miele, O. Pisanti, and P. D. Serpico, Phys. Rep. **472**, 1 (2009).
[54] Y. I. Izotov and T. X. Thuan, Astrophys. J. **710**, L67 (2010).
[55] E. Aver, K. A. Olive, and E. D. Skillman, J. Cosmol. Astropart. Phys. 05 (2010) 003.
[56] E. Aver, K. A. Olive, and E. D. Skillman, J. Cosmol. Astropart. Phys. 03 (2011) 043.
[57] E. Aver, K. A. Olive, and E. D. Skillman, J. Cosmol. Astropart. Phys. 04 (2012) 004.
[58] G. Mangano and P. D. Serpico, Phys. Lett. B **701**, 296 (2011).
[59] M. Pettini and R. Cooke, arXiv:1205.3785.
[60] P. D. Serpico and G. G. Raffelt, Phys. Rev. D **71**, 127301 (2005).
[61] J. Lesgourgues, L. Perotto, S. Pastor, and M. Piat, Phys. Rev. D **73**, 045021 (2006).
[62] http://lpsc.in2p3.fr/perotto/.
[63] L. Perotto, J. Lesgourgues, S. Hannestad, H. Tu, and Y. Y. Y. Wong, J. Cosmol. Astropart. Phys. 10 (2006) 013.